Tumor-Targeting Properties of Novel Antibodies Specific to the Large Isoform of Tenascin-C

Simon S. Brack,[1] Michela Silacci,[1] Manfred Birchler,[2] and Dario Neri[1]

Abstract

Background: The targeted delivery of bioactive molecules with antibodies specific to tumor-associated antigens represents a promising strategy for improving the efficacy of tumor therapy. The large isoform of tenascin-C, an abundant glycoprotein of the tumor extracellular matrix, is strongly overexpressed in adult tissue undergoing tissue remodeling, including wound healing and neoplasia, and has been implicated in a variety of different cancers while being virtually undetectable in most normal adult tissues.

Experimental Design: We have used antibody phage technology to generate good-quality human recombinant antibodies (F16 and P12) specific to the alternatively spliced domains A1 and D of the large isoform of tenascin-C. The tumor-targeting properties of F16 and P12 were assessed by biodistribution studies in tumor xenografts using the antibodies in small immunoprotein (SIP) format.

Results: SIP(F16) selectively accumulated at the tumor site with 4.5%ID/g at 24 hours in the U87 glioblastoma model but was rapidly cleared from other organs (tumor-to-organ ratios, ~10:1). The accumulation of SIP(P12) in the tumor was lower compared with SIP(F16) and persistent levels of radioactivity were observed in the intestine.

Conclusions: These data suggest that the F16 antibody, specific to domain A1 of tenascin-C, is a promising building block for the development of antibody-based pharmaceuticals in view of its excellent tumor-targeting performance and the strong expression of the antigen in a variety of primary and metastatic tumors.

A promising avenue toward the development of more selective anticancer therapies consists in the targeted delivery of bioactive molecules (antibody constant regions, cytokines, drugs, radionuclides, photosensitizers, procoagulant factors, etc.) to the tumor environment by means of ligands specific to good-quality tumor-associated antigens and endowed with suitable pharmacokinetic properties (1–7).

Antigens that are preferentially expressed in the modified tumor extracellular matrix are, in many respects, ideal targets for tumor-targeting applications (2, 8). Extracellular matrix components are often more abundant and more stable than antigens located on the surface of tumor cells. Furthermore, they typically exhibit a low shedding profile and are well accessible to agents (such as antibody derivatives) coming from the bloodstream. In collaboration with the Zardi group (Genova, Italy), our group has extensively shown the tumor-targeting potential of antibodies directed against components of the tumor extracellular matrix using, as an example, the L19 human monoclonal antibody (9), specific to the extradomain B of fibronectin (EDB), a marker of angiogenesis (10–12). The L19 antibody was shown to efficiently target tumor neovasculature and stromal structures in animal models of cancer (13) and in patients with aggressive solid tumors (14). Furthermore, several therapeutic derivatives of the antibody fragment single-chain Fv (scFv) L19 [scFv(L19)] have been tested in animal models of cancer (15–22). At present, the therapeutic properties of ^{131}I-small immunoprotein (SIP) L19 [SIP(L19); refs. 23, 24] and scFv(L19)-IL2 (15, 25) are being investigated in clinical trials.

The EDB domain of fibronectin is a good-quality marker of angiogenesis, which is overexpressed in a variety of solid tumors (renal cell carcinoma, colorectal carcinoma, hepatocellular carcinoma, high-grade astrocytomas, head and neck tumors, bladder cancer, etc.). However, EDB is only weakly expressed in most forms of breast cancer (12), prostate cancer, and some types of lung cancer, thus stimulating the search for novel vascular tumor antigens, which could be used for the antibody-mediated targeted delivery of therapeutic cytokines to these neoplasias. In principle, splice isoforms of tenascin-C could be considered as targets for antibody-based therapeutic strategies, particularly for those tumor classes in which low levels of EDB can be detected.

Authors' Affiliations: [1]Institute of Pharmaceutical Sciences, Department of Chemistry and Applied Biosciences, Swiss Federal Institute of Technology Zürich; and [2]Stadtspital Triemli, Chirurgische Klinik ORL, Zürich, Switzerland

Received 12/22/05; revised 2/22/06; accepted 3/8/06.

Grant support: Swiss Federal Institute of Technology Zurich, Swiss National Science Foundation, Bundesamt für Bildung und Wissenschaft (EU Project STROMA), and Philogen SpA.

The costs of publication of this article were defrayed in part by the payment of page charges. This article must therefore be hereby marked *advertisement* in accordance with 18 U.S.C. Section 1734 solely to indicate this fact.

Note: Supplementary data for this article are available at Clinical Cancer Research Online (http://clincancerres.aacrjournals.org/).

Requests for reprints: Dario Neri, Institute of Pharmaceutical Sciences, Department of Chemistry and Applied Biosciences, Swiss Federal Institute of Technology Zürich, Wolfgang-Pauli-Strasse 10, CH-8093 Zürich, Switzerland. Phone: 41-44-633-74-01; Fax: 41-44-633-13-58; E-mail: neri@pharma.ethz.ch.

doi:10.1158/1078-0432.CCR-05-2804

Tenascin-C is a glycoprotein of the extracellular matrix. It comprises several fibronectin type 3 homology repeats that can be either included or omitted in the primary transcript by alternative splicing, leading to small and large isoforms that have distinct biological functions (refs. 26, 27; Fig. 1A). Whereas the small isoform is expressed in several tissues, the large isoform of tenascin-C exhibits a restricted pattern of expression. It is virtually undetectable in healthy adult tissues but is expressed during embryogenesis and is reexpressed in adult tissues undergoing tissue remodeling including neoplasia. Its expression is localized around vascular structures in the tumor stroma of a variety of different tumors, including breast carcinoma (26), oral squamous cell carcinoma (28), lung cancer (29), prostatic adenocarcinoma (30), colorectal cancer (31), or astrocytoma and other brain tumors (32, 33).

Traditionally, one has referred to the large isoform of tenascin-C for tenascin molecules, which would putatively comprise all alternatively spliced domains, and to the small isoform of tenascin-C whenever these domains were absent. Carnemolla et al. have reported that the alternatively spliced domain C of tenascin-C exhibited a more restricted pattern of expression compared with other alternatively spliced domains (32). It remained unclear at that time whether other alternatively spliced domains of tenascin-C also exhibited restricted incorporation into the tenascin molecule and whether it would be more appropriate to evaluate the individual spliced domains separately as targets for antibody-based therapeutic strategies.

Radiolabeled antibodies specific to domains A1 and D of tenascin-C have been successfully used in the clinic for the treatment of glioma and of lymphoma (34–36). Furthermore, efficient tumor targeting by anti-tenascin antibodies has been shown clinically using an avidin/biotin-based pretargeting approach (37) or, more recently, with monoclonal antibodies specific for the small isoform of tenascin-C (38, 39). However, all these antibodies are of murine origin and may therefore not be suitable for repeated administration to patients and for the development of biopharmaceuticals. For these reasons, we have generated human antibodies specific to domains A1 and D of tenascin-C using antibody phage technology (40). Considering that antibodies isolated from nonimmune libraries often exhibit binding affinities, which are insufficient for *in vivo* use, these antibodies were affinity matured and evaluated in

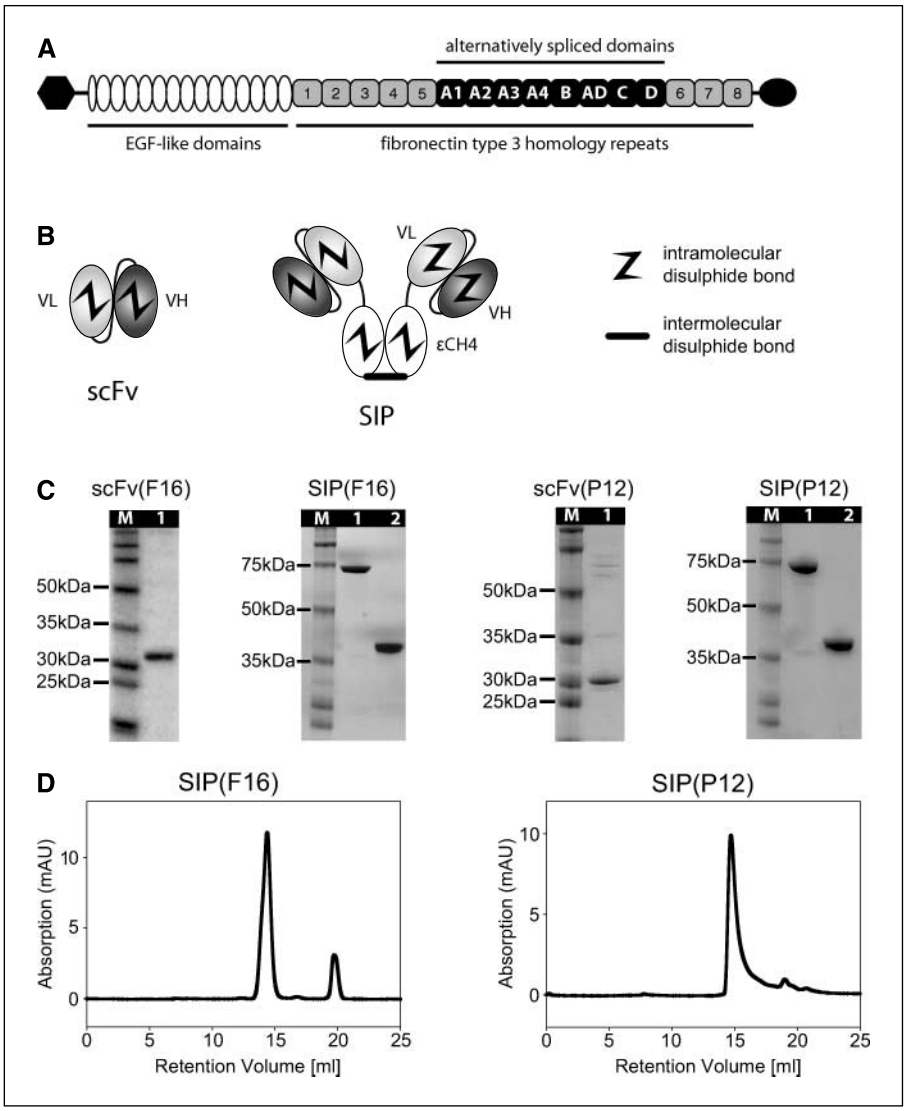

Fig. 1. Antibodies against the large isoforms of tenascin-C. *A,* structural model of one subunit of tenascin-C. Structural domains: hexagon, tenascin assembly domain; ellipses, epidermal growth factor (*EGF*) – like repeats; gray squares, constant fibronectin type 3 homology repeats; black squares, alternatively spliced fibronectin type 3 homology repeats; circle, fibrinogen globe. *B,* schematic illustration of the scFv format consisting of a heavy chain (*VH*) and a light chain (*VL*) linked by a peptide linker and schematic illustration of the SIP format consisting of a disulfide linked homodimer. *C,* SDS-PAGE of affinity-purified anti-TnC-A1 antibodies scFv(F16) and SIP(F16) and affinity-purified anti-TnC-D antibodies scFv(P12) and SIP(P12). Lane 1, SIP antibodies under nonreducing condition; lane 2, SIP antibodies under reducing conditions. M, molecular weight marker. *D,* size exclusion chromatogram of SIP(F16) and of SIP(P12) on a Superdex 200 HR10/30 column. The major peak eluting at ~14.5 mL corresponds to the molecular weight of the dimer. The minor peak at 19.7 mL in the chromatogram of SIP(F16) derives from contaminating DNA.

quantitative biodistribution studies in a mouse model of glioblastoma using radioiodinated protein preparations, confirming that the extradomain A1 of tenascin-C is a suitable antigen for antibody-based tumor-targeting applications.

Materials and Methods

Selections of antibodies from the ETH-2 library by phage display. Panning of the ETH-2 library with biotinylated recombinant antigens, either human domain A1 of tenascin-C (TnC-A1) or human domain D of tenascin-C (TnC-D), was done essentially as described by Viti et al. (41). In brief, antigens were biotinylated using EZ-link sulfo-NHS-SS-biotin (Pierce, Rockford, IL) and the biotinylated antigen was incubated at 10^{-7} mol/L concentration with 10^{12} transforming units of phage antibodies. The phage-antigen complex was then captured using streptavidin-coated magnetic beads (Dynal, Oslo, Norway). The beads were washed with 0.1% Tween 20 in PBS and with PBS [100 mmol/L NaCl, 50 mmol/L phosphate (pH 7.4)]. Bound phage was eluted with DTT (Applichem, Darmstadt, Germany) and amplified in *Escherichia coli* TG-1 using VCS-M13 (Stratagene, La Jolla, CA) as helper phage. Phage particles were purified from culture supernatant by polyethylene glycol precipitation (41). Three rounds of panning were done for both antigens.

Screening of supernatants by ELISA, BIAcore, and competition ELISA. Induced supernatants of individual clones were screened by ELISA as described by Viti et al. (41) on high-bind StreptaWell plates (Roche, Mannheim, Germany) coated with biotinylated antigen. Bound antibody was detected by means of anti-peptide tag antibodies, either anti-myc tag antibody 9E10 or anti-Flag tag antibody M2 (Sigma, Steinheim, Germany), followed by an anti-mouse immunoglobulin horseradish peroxidase conjugate (Sigma). Supernatants of ELISA-positive clones were further screened by surface plasmon resonance real-time interaction analysis on a high-density coated antigen chip, using a BIAcore3000 instrument (BIAcore AB, Uppsala, Sweden), and by M2 competition ELISA as described by Scheuermann et al. (42).

Sequencing of scFv antibody genes. Antibodies were sequenced using Big Dye Terminator version 1.1 Cycle Sequencing kit (Applied Biosystems, Foster City, CA) on an ABI PRISM 3130 Genetic Analyzer. Primers used for sequencing were LMB3 long (5′-CAGGAAACAGCTATGACCATGATTAC-3′; annealing upstream of scFv gene), fdseq long (5′-GACGTTAGTAAATGAATTTTCTGTATGAGG-3′, annealing downstream of scFv gene), and DP47CDR2ba [5′-ACATACTACGCAGACTCCGTGAAGGGC-3′, annealing 100 bp upstream of variable heavy chain (VH) CDR3].

Characterization of scFv antibodies. scFv antibody fragments were expressed in *E. coli* TG-1 and purified from culture supernatant and from periplasmic preparations by affinity chromatography using either protein A-Sepharose (Amersham Biosciences, Uppsala, Sweden) or antigen-coupled Sepharose obtained by coupling recombinant antigen to CnBr-activated Sepharose (Amersham Biosciences).

Purified antibodies were analyzed by size exclusion chromatography on Superdex 75 HR10/30 columns (Amersham Biosciences); peaks representing monomeric fractions were collected and used for affinity measurements by BIAcore on a low-density coated antigen chip.

Immunohistochemistry on frozen tissue sections. Sections of 8- to 12-μm thickness were treated with ice-cold acetone, rehydrated in TBS [50 mmol/L Tris, 100 mmol/L NaCl (pH 7.4)], and blocked with 20% fetal bovine serum (Invitrogen, Basel, Switzerland). Affinity-purified scFv fragments (final concentration, 2-10 μg/mL) carrying either a Flag tag or a myc tag were added onto the sections together with a secondary antibody, which was either monoclonal anti-Flag antibody M2 or monoclonal anti-myc 9E10 antibody (5 μg/mL). Bound antibodies were detected with rabbit anti-mouse immunoglobulin antibody (Dakocytomation, Glostrup, Denmark) followed by mouse monoclonal alkaline phosphatase-anti-alkaline phosphatase complex (Dakocytomation). Fast Red (Sigma) was used as phosphatase substrate, and sections were counterstained with Gill's hematoxylin no. 2 (Sigma).

Immunohistochemistry with SIP antibodies was done as with scFv antibody fragments; however, bound SIP antibody was detected with rabbit anti-human IgE antibody (Dakocytomation) followed by biotinylated goat anti-rabbit IgG antibody (Biospa, Milan, Italy) and streptavidin-alkaline phosphatase complex (Biospa).

Affinity maturation of scFv(D5). The affinity maturation library was cloned by introducing mutations in the VH CDR1 residues 31 to 34 [numbering according to Chothia/Tomlinson et al. (43)] of scFv(D5) with partially degenerate primers DP47CDR1for (5′-AGCCTGGCGGACCCAGCTCATMNNMNNMNNGCTAAAGGTGAATCCAGAGGCTGC-3′; M designates wobble A or C and N designates wobble A, C, G, or T), DP47CDR1formut (5′-AGCCTGGCGGACCCAGCTCGCMNNMNNMNNGCTAAAGGTGAATCCAGAGGCTGC-3′), and DP47CDR1ba (5′-GAGCTGGGTCCGCCAGGCTCC-3′). Gel-purified PCR fragments were assembled to full-length insert by PCR; the resulting fragment was digested with *Nco*I and *Not*I (New England Biolabs, Beverly, MA) and cloned into *Nco*I/*Not*I-digested pDNEK vector (9). The ligation was electroporated into *E. coli* TG-1, and phages were rescued by superinfection with helper phage VCS-M13. The resulting library was used for two rounds of panning using 10^{-8} mol/L biotinylated human TnC-A1 as antigen. Screening and characterization was done by ELISA, size exclusion chromatography, and BIAcore as described above.

Affinity maturation of scFv(F4). Random mutations at variable light chain (VL) CDR1 positions 31a, 31b, and 32 and VL CDR2 positions 50, 52, and 53 [numbering according to Chothia/Williams et al. (44)] were introduced into scFv(F4) by PCR using primers DPL16CDR1fo (5′-TCCTGGCTTCTGCTGGTACCAGCTTGCMNNMNNMNNTCTGAGGCTGTCTCCTTG-3′), DPL16CDR1ba (5′-TGGTACCAGCAGAAGCCAGGA-3′), DPL16CDR2fo (5′-GTCTGGGATCCCTGAGGGCCGMNNMNNTTTMNNATAGATGACAAGTACAGGGGCC-3′), and DPL16CDR2ba (5′-CGGCCCTCAGGGATCCCAGAC-3′). The resulting PCR fragments were purified by agarose gel electrophoresis and assembled by PCR. The resulting fragment was digested by *Nco*I and *Not*I and cloned into vector pHEN1 (45). After ligation, the constructs were electroporated into freshly prepared *E. coli* TG-1 cells, yielding 3×10^8 colonies, which is four times more than the theoretical library size (6.4×10^7). Phages were produced form these cells as described above. Two rounds of selections using 10^{-8} mol/L biotinylated human TnC-D in the first round and 10^{-8} mol/L biotinylated mouse TnC-D in the second round were done. Clones were screened and characterized as described above.

Affinity maturation of scFv(D11). The scFv(D11) affinity maturation library carrying random mutations in the scFv(D11) gene at VH CDR1 positions 31, 32, and 33 and VH CDR2 positions 52, 52a, 53, and 56 [numbering according to Chothia/Tomlinson et al. (43)] was obtained similar to the scFv(F4) affinity maturation library using the primers DP47CDR1(D11)fo (5′-CTGGAGCCTGGCGGACCCAGCTCATMNNMNNMNNGCCAAAGGTGAATCCAGAGGCTGC-3′), DP47CDR1(D11)ba (5′-TGGGTCCGCCAGGCTCCAG-3′), DP47CDR2(D11)fo (5′-GCCCTCCACGGAGTCTGCGTAGTATGTMNNACCACCMNNMNNMNNAATAGCTGAGACCCACTCC-3′), and DP47CDR2(D11)ba (5′-ACATACTACGCAGACTCCGTGGAGGGC-3′). The obtained library comprised 8.5×10^8 colonies (theoretical library size, 1.3×10^9). The library was subjected to two rounds of panning using 10^{-8} mol/L biotinylated human TnC-D as antigen. Screening and characterization was done as described above.

Cloning, expression, and purification of SIP proteins. The SIP secretion sequence, which is required for secretion into the extracellular medium, was amplified from the construct SIP(L19)-pcDNA3.1 (23) using primers 23sbba (5′-CCAATTCTGAAGCTTGTCGACCATGGGCTG-3′) and 29sbfo (5′-CAGCTGCACCTCCGAGTGCACACCTGTGGAGAG-3′). The human εCH4 domain was amplified from the same construct using primers 34sbba (5′-ACCGTCCTAGGCTCCGGAGGCTCTGGGGGCC-3′) and 28sbfo (5′-CTGGAATTCGAGCTCGGTACCTAGCAGC-3′). scFv were amplified with 30sbba (5′-GGTGTGCACTCGGAGGTGCAGCTGTTGGAGTCT-3′) for scFv(F16) or 30sbba_P12

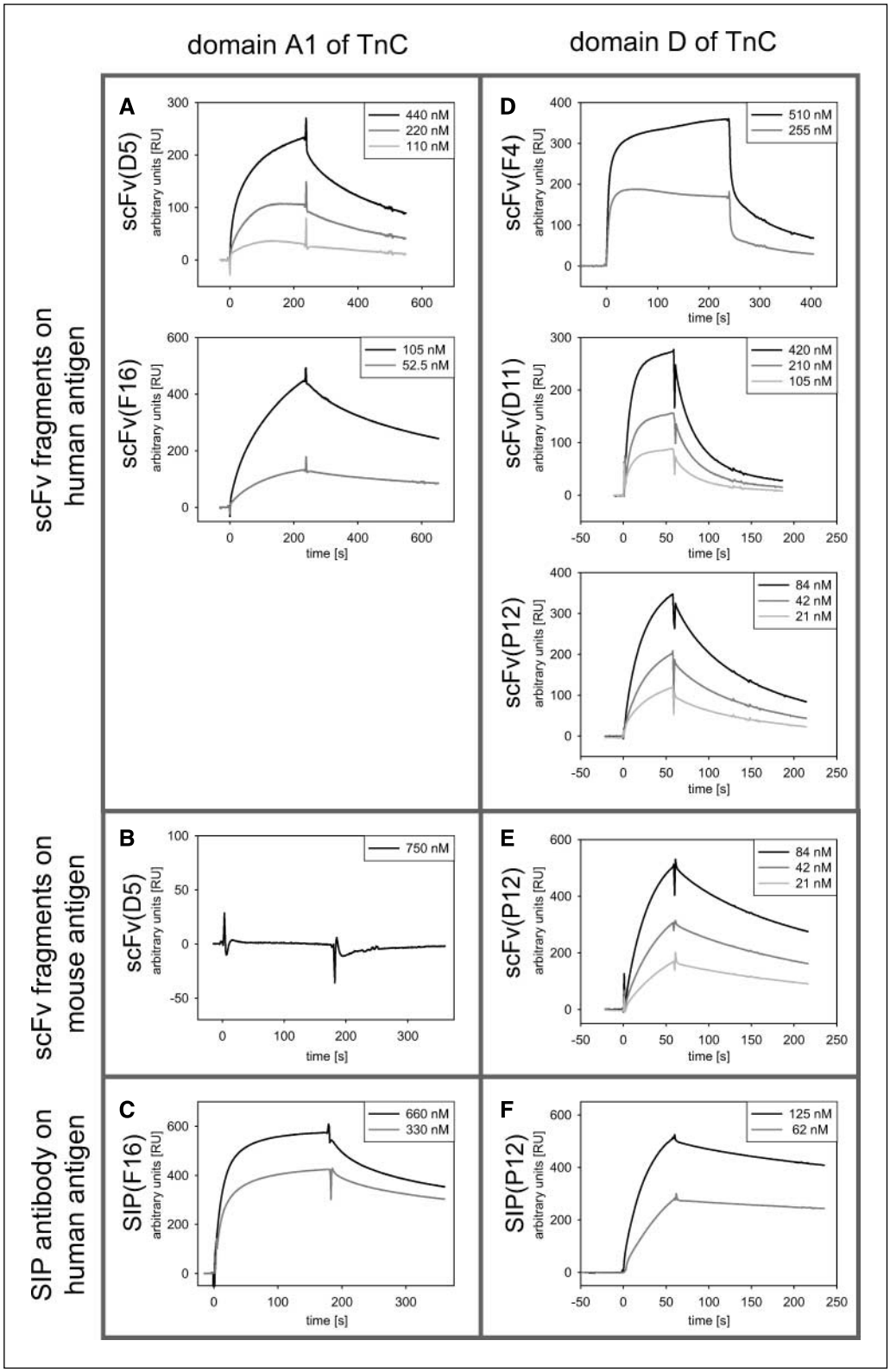

Fig. 2. BIAcore sensograms of anti-tenascin-C antibodies at different concentrations. *A,* monomeric fractions of scFv(D5) (*top*) and affinity-matured scFv(F16) (*bottom*) on human TnC-A1. *B,* scFv(D5) on mouse TnC-A1 shows no binding. *C,* SIP(F16) on human TnC-A1. *D,* monomeric fractions of scFv(F4) (*top*) and affinity-matured antibodies scFv(D11) (*middle*) and scFv(P12) (*bottom*) on human TnC-D. *E,* monomeric fractions of scFv(P12) on mouse TnC-D. *F,* SIP(P12) on human TnC-D.

(5′-GGTTCACTCGGAGGTGCAGCTGGTGGAGTCT-3′) for scFv(P12), respectively, and 33sbfo (5′-CCCGGCCTCCGGAGCCTAGGACG-GTCAGCTTGGT-3′). The resulting PCR fragments were gel purified, assembled by PCR, and cloned into vector pcDNA3.1 (Invitrogen) by means of *Hin*dIII and *Eco*RI digestion.

The constructs were used to transfect HEK293 cells using FuGENE 6 transfection reagent (Roche). Transfected HEK293 cells were grown in DMEM (Invitrogen) supplemented with 10% fetal bovine serum (Invitrogen) and selected using 500 μg/mL geneticin (G418, Calbiochem, La Jolla, CA). Monoclonal cultures were obtained by limited

Table 1. Amino acid sequence of anti-tenascin-C antibodies at relevant positions

Antigen	Clone	VH chain			VL chain		
		31-34	52-56	95-98	31a-32	50-53	92-95b
TnC-A1	D5	SYAA	SGSGGS	*AHNA*	SYY	GKNN	*VYTMPP*
	F16	**RYGA**	SGSGGS	*AHNA*	SYY	GKNN	*VYTMPP*
TnC-D	F4	SYAM	SGSGGS	*GRRI*	SYY	GKNN	*SPKPKP*
	D11	SYAM	SGSGGS	*GRRI*	**RQP**	**YKKL**	*SPKPKP*
	P12	**QYS**M	**TGT**GGE	*GRRI*	RQP	YKKL	*SPKPKP*

NOTE: Sequences are given in single-letter amino acid code. Italicized residues in the CDR3 of VH and VL have been mutated in the ETH-2 library; residues in boldface have been mutated for affinity maturation. Numbering is according to Chothia (48, 49).

dilution. SIP antibodies were purified from supernatant by affinity chromatography using antigen-coated Sepharose resin. The purified proteins were analyzed by SDS-PAGE, size exclusion chromatography using a Superdex 200 HR10/30 column, and BIAcore.

Biodistribution in U87 human glioblastoma model. U87 human glioblastoma cells (3×10^6; HTB-14, American Type Culture Collection, Manassas, VA) were injected s.c. into the right flank of 6- to 8-week-old female BALB/c *nu/nu* mice (Charles River Laboratories, Wilmington, MA). The tumors were allowed to grow for 20 to 25 days. By then, tumors reached a size of typically 200 mg and were used for biodistribution studies.

The *in vivo* targeting performance of the SIP antibodies was evaluated by biodistribution analysis as described by Tarli et al. (13). Briefly, purified SIP antibodies were radioactively labeled with ^{125}I using Iodo-Gen (Pierce) and injected i.v. into tumor-bearing mice. The amounts injected were 5 μg SIP(F16) and 3.5 μg SIP(P12). Animals were sacrificed 3, 6, 24, and 48 hours after injection, respectively. Organs were excised and weighed and the radioactivity was counted. Targeting results of representative organs are expressed as %ID/g tissue. For the side-by-side comparison of SIP(F16) and SIP (L19), mice were sacrificed and analyzed 24 hours after injection of 2.7 μg SIP(F16) and 5.4 μg SIP(L19).

Results

Isolation and characterization of scFv antibody fragments specific to domains A1 and D. Monoclonal antibodies were isolated from the synthetic human scFv antibody library ETH-2 by phage display (9) using TnC-A1 or TnC-D as antigen. Several clones that were positive in ELISA and BIAcore were tested by immunohistochemistry for their ability to recognize the antigen in the tissue on tumor xenograft sections. Finally, several clones were purified by affinity chromatography and characterized by size exclusion chromatography. Monomeric fractions were collected and used for affinity measurements by BIAcore on a low-density antigen-coated chip. This led to the identification of the anti-TnC-A1 antibody scFv(D5) and the anti-TnC-D antibody scFv(F4) (Fig. 2A and D; Table 1; Supplementary Table S1). Both antibodies bound to their antigen in a highly specific manner and did not cross-react with any of eight other structurally related fibronectin type 3 homology repeats of either tenascin-C, tenascin-R, or fibronectin as determined by ELISA (Fig. 3). Whereas scFv(F4) reacted with TnC-D of both human and murine origin, we failed to isolate antibody clones recognizing both human and murine versions of TnC-A1, which share 78% sequence identity.

In vitro *affinity maturation of ETH-2 antibodies.* To improve the binding properties of scFv(D5) and scFv(F4), *in vitro* affinity maturation was done by mutation of residues in the CDR1 and CDR2 of the antibody heavy and/or light chains as described by Pini et al. (9). This approach is particularly well suited for clones from the ETH-2 or the ETH-2 Gold library (9, 46), because these libraries consist of clones with combinatorial diversity concentrated in the CDR3 loops, whereas the rest of the antibody gene is conserved for all library members (9, 46). scFv(D5) was affinity matured by introducing random mutations, which allow all 20 amino acids at three positions within the VH CDR1. Because residue 34 in the VH CDR1 was mutated from methionine in the germ-line gene DP47 to alanine in scFv(D5), we mutated this position allowing both alanine and methionine. The best clone isolated from the resulting affinity maturation library, scFv(F16), had an affinity improvement by a factor 3 compared with scFv(D5) (Fig. 2A; Table 1; Supplementary Table S1).

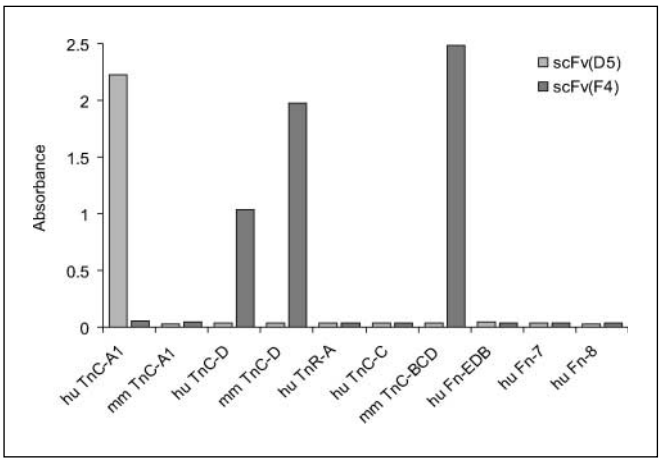

Fig. 3. Specificity of anti-TnC-A1 antibody scFv(D5) and anti-TnC-D antibody scFv(F4). ELISA signals on different fibronectin type 3 homology repeats, showing that both antibodies specifically recognize the cognate antigen [i.e., human domain TnC-A1 for scFv(D5) or human and mouse TnC-D for scFv(F4)]. scFv(D5) did not react with mouse TnC-A1. huTnC-A1, human domain A1 of tenascin-C; mmTnC-A1, mouse domain A1 of tenascin-C; huTnC-D, human domain D of tenascin-C; mm TnC-D, mouse domain D of tenascin-C; huTnR-A, human domain A of tenascin-R; huTnC-C, human domain C of tenascin-C; mmTnC-BCD, mouse domains BCD of tenascin-C; hu Fn-EDB, human EDB; hu Fn-7, human domain 7 of fibronectin; hu Fn-8, human domain 8 of fibronectin.

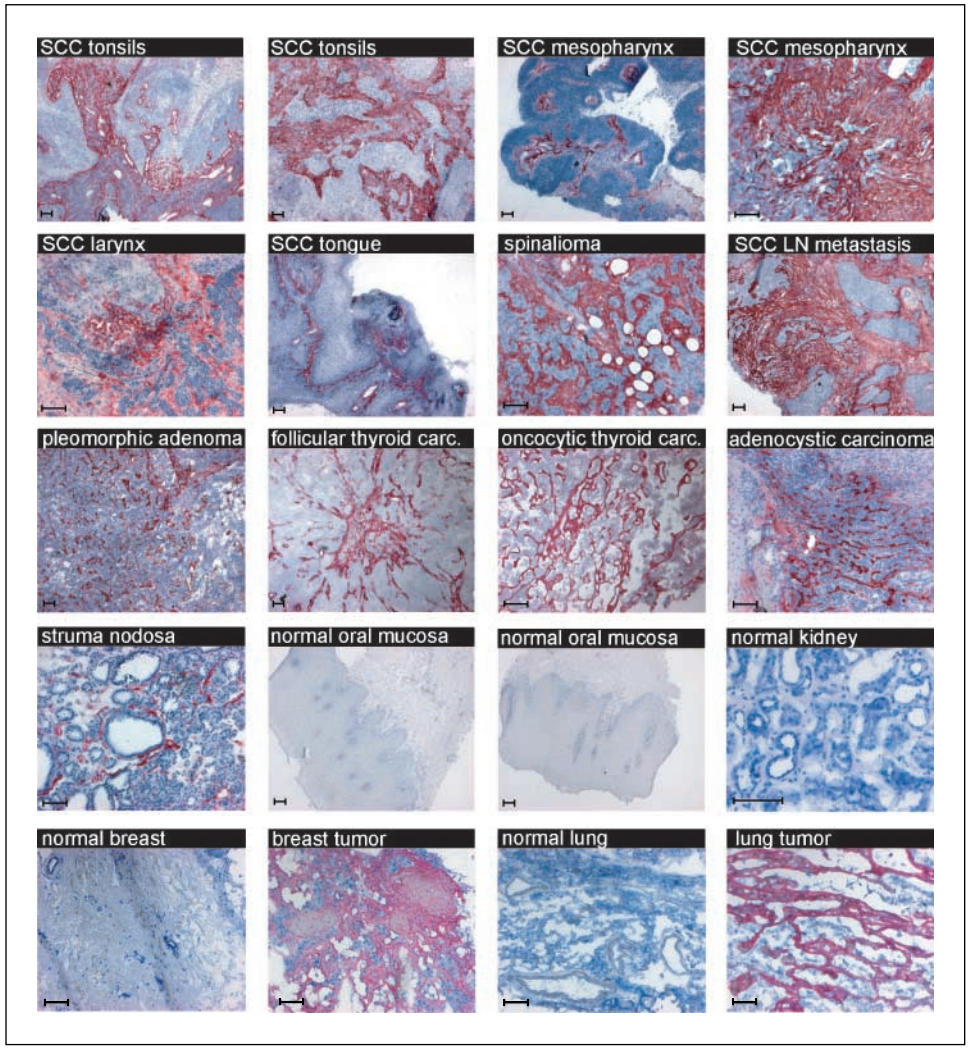

Fig. 4. Immunohistochemistry with scFv(D5) on human head and neck, breast, and lung tumor sections and on normal tissue sections. All sections presented were from different donors. SCC, squamous cell carcinoma; LN, lymph node. Bar, 100 μm.

scFv(F4) was affinity matured in two steps. First, random mutations were introduced at six positions within the VL CDR1 and VL CDR2, leading to an intermediate anti-TnC-D antibody scFv(D11) (Fig. 2D; Table 1; Supplementary Table S1). Further improvement was achieved by targeting random mutations to seven positions within the VH CDR1 and VH CDR2. The best clone isolated from this second library, scFv(P12), showed an affinity improvement by a factor 11 to human TnC-D compared with scFv(F4) (Fig. 2D; Table 1; Supplementary Table S1). scFv(P12) also bound with high affinity to the mouse isoform of TnC-D (Fig. 2E; Supplementary Table S1).

Immunohistochemistry with scFv(D5) on human tissue sections. scFv(D5) was extensively characterized by immunohistochemistry on cryosections of human head and neck tumors. The tumor stroma and neovascular structures were intensely stained, proving that scFv(D5) recognized the cognate antigen in its native conformation (Fig. 4). TnC-A1 was shown to be prominently expressed in several carcinomas, including different-stage primary squamous cell carcinoma of the tongue, tonsils, mesopharynx/hypopharynx, or larynx, as well as lymph node metastases. One of two adenocarcinomas examined was positive for TnC-A1, which agrees with the suggestion that the expression of large isoforms of tenascin-C correlates with invasiveness (47, 48). Structures of the thyroid of a patient suffering from struma nodosa were also positively stained for TnC-A1. scFv(D5) did not stain normal mucosa from two different healthy donors, normal kidney, normal breast, or normal lung, confirming the specificity of this antigen (Fig. 4). Moreover, unlike anti-EDB antibodies, scFv(D5) strongly reacted with lung tumor and breast tumor specimens.

Immunohistochemistry on tumor xenograft sections. Expression of TnC-A1 and TnC-D in different mouse tumor models was examined by immunohistochemistry using the different antibodies generated and was compared with expression of the EDB by means of the L19 antibody (9, 14).

Tumor cells were injected s.c. into nude mice (A375 human melanoma and U87 human glioblastoma, American Type Culture Collection) or immunocompetent SvEv 129 mice (murine F9 teratocarcinoma, American Type Culture Collection). After 8 days (F9), 20 days (U87), or 30 days (A375), when tumors reached volumes of >200 mm^3, they were excised and frozen sections were prepared, which were stained with the relevant antibodies. All antibodies gave similar stainings on both A375 and U87 (Fig. 5). Murine F9 teratocarcinoma was strongly positive around blood vessels for TnC-D as for EDB (Fig. 5).

Production of antibodies SIP(F16) and SIP(P12). The antibodies scFv(F16) and scFv(P12) were cloned into the SIP

format by genetically fusing the scFv at the NH_2 terminus of a human εCH4 domain of the secretory isoform S2 of human IgE (23). This domain promotes the formation of homodimers that are further stabilized by disulfide bonds between the COOH-terminal cysteine residues, resulting in a 75-kDa bivalent mini-antibody (Fig. 1). This format is superior to IgG and to scFv in achieving high tumor-to-organ ratios (23) and for radio-immunotherapeutic applications (24). IgGs exhibit high tumor levels due to their long circulation half-life and due to their bivalent nature, but they also display high blood levels because of a slow clearance. In contrast, scFv are rapidly cleared from blood and organs, which leads to decreased tumor accumulation compared with IgG. The SIP format offers a good compromise between high tumor uptake and fast elimination from the blood and from organs (see also refs. 49, 50). Furthermore, the bivalent nature of SIP mini-antibodies leads to improved functional affinity due to avidity effects compared with their monomeric scFv counterparts (Fig. 2C and F). SIP antibodies lack the ability to interact with the high-affinity IgE receptor (which is mediated by the εCH3 domain) and therefore do not pose safety concerns.

The recombinant antibodies SIP(F16) and SIP(P12) were expressed in human embryonic kidney cells (HEK293) from a pcDNA3.1-based expression vector and purified by affinity chromatography from cell culture supernatant (Fig. 1C). Both proteins were characterized by quantitative formation of disulfide-bonded homodimers and were resistant to aggregation as shown by SDS-PAGE and size exclusion chromatography (Fig. 1D), confirming the high stability of SIP antibodies. Indeed, SIP(F16) exhibited a reproducible gel filtration profile even after storage for 10 months at 4°C (data not shown).

Tumor-targeting studies with SIP(F16) and SIP(P12) in tumor-bearing mice. The *in vivo* targeting performance of SIP(F16) and SIP(P12) was evaluated by biodistribution experiments in U87 human glioblastoma xenograft-bearing nude mice. ^{125}I-labeled SIP antibodies were injected i.v. After 3,

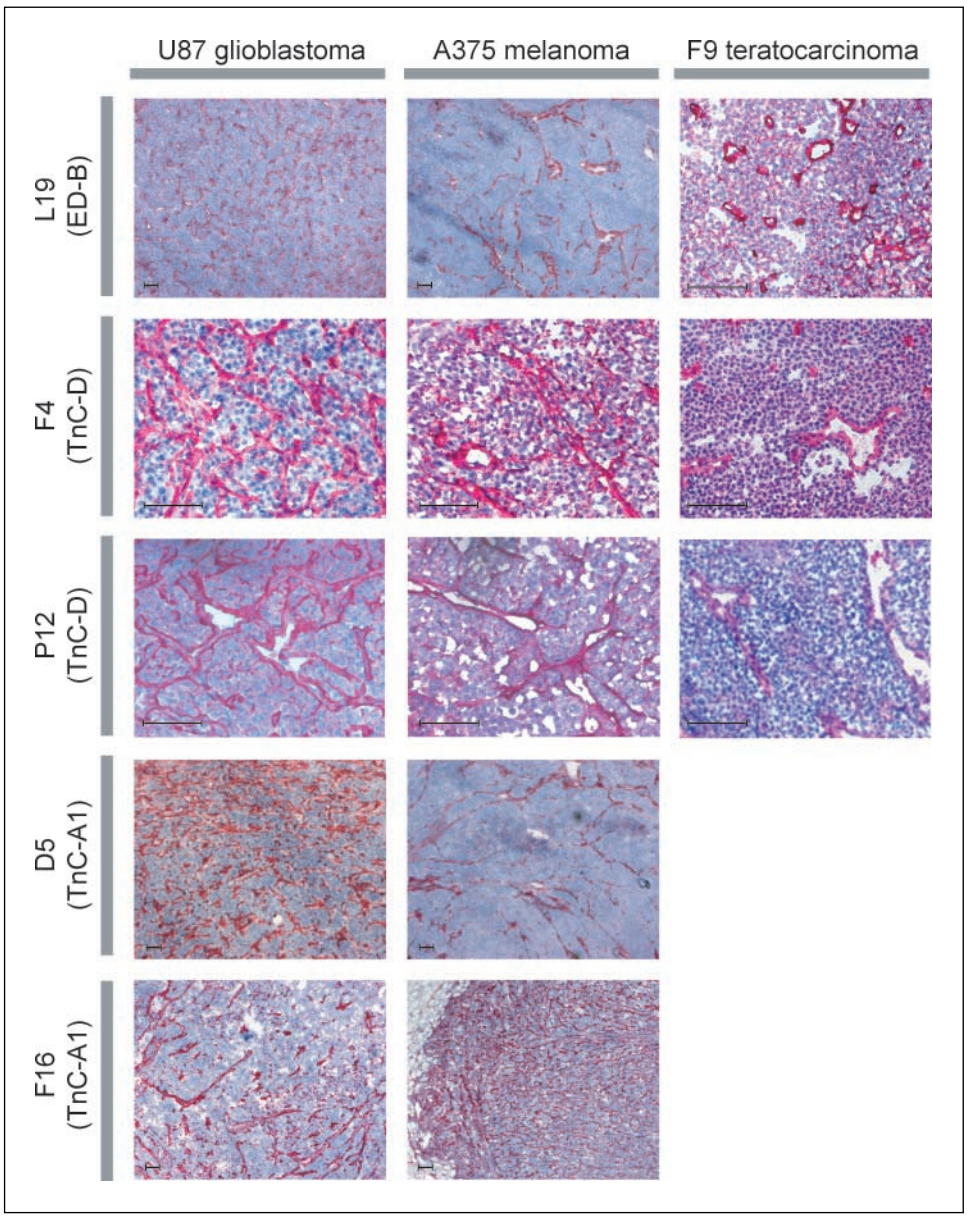

Fig. 5. Immunohistochemistry with relevant antibodies on different mouse cancer models. Left, U87 human glioblastoma; middle, A375 human melanoma; right, F9 murine teratocarcinoma. The sections were stained for EDB with L19, forTnC-D with F4 and P12, and forTnC-A1 with D5 and F16. As expected, D5 and F16 did not give any staining on murine F9 teratocarcinoma (data not shown). Bar, 100 μm.

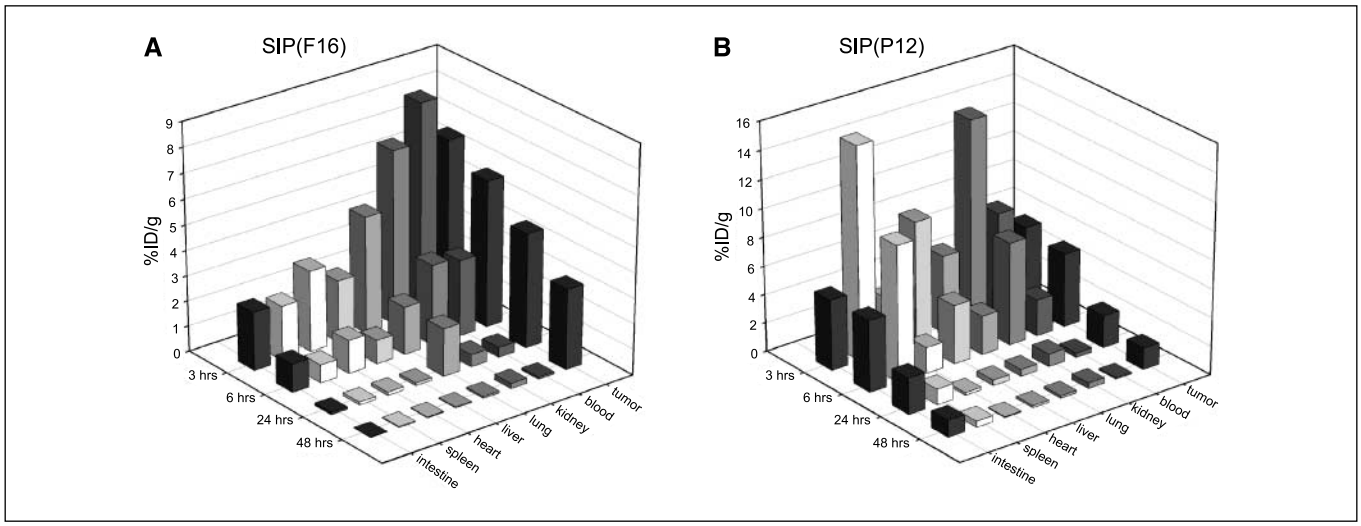

Fig. 6. Biodistribution of SIP(F16) and SIP(P12) in U87-bearing nude mice at four different time points after i.v. injection. *A,* biodistribution of ^{125}I-labeled SIP(F16). Each time point corresponds to an average of three animals. *B,* biodistribution of ^{125}I-labeled SIP(P12). Each time point corresponds to an average of four animals. Results are expressed as %ID/g tissue.

6, 24, and 48 hours, animals were sacrificed, organs were excised and weighed, and radioactivity was counted.

SIP(F16) selectively accumulated at the tumor site and was cleared within a few hours from blood and from other organs. Values in the tumor remained high even 48 hours after injection, resulting in tumor-to-blood ratios of up to 40 (Fig. 6A; Supplementary Table S2).

SIP(P12) was cleared within 24 hours after injection from most organs, and specific accumulation at the tumor site was observed after 24 and 48 hours, with tumor-to-blood ratios of up to 15. However, the retention of the antibody in the tumor was less efficient than for SIP(F16). Moreover, values in the intestine remained at a relatively high level, which were comparable with tumor values (Fig. 6B; Supplementary Table S3).

We did a side-by-side comparison of the tumor-targeting performance of SIP(F16) and SIP(L19) in the U87 glioblastoma model. SIP(F16) did at least as well as SIP(L19), with similar antibody levels in the tumor and slightly lower levels in the organs after 24 hours (Supplementary Fig. S1).

Discussion

We have examined the tumor-targeting performance of two antibodies specific to two different epitopes of the large tenascin-C isoform. Both antibodies were isolated from the ETH-2 library (9) by phage display and affinity matured *in vitro* by randomization of several residues located in the CDR1 and CDR2 of the heavy and/or light chains. The affinities that were reached after affinity maturation were in the two-digit nanomolar range for both clones.

The anti-TnC-A1 antibody SIP(F16) accumulated specifically at the tumor site and targeted tumors with a performance that was comparable with the one of SIP(L19), a high-affinity antibody directed toward the EDB, which is currently in phase II clinical trials. Because the antibody F16 does not cross-react with the murine isoform of domain A1, it fails to detect antigen expressed in mouse organs. This should be taken into account when interpreting biodistribution results, particularly for organ levels and for tumor-to-organ ratios, which were slightly better than the ones of SIP(L19) (Supplementary Fig. S1).

Whereas the anti-TnC-A1 antibody SIP(F16) specifically accumulated in the tumor, the anti-TnC-D antibody SIP(P12) did less well and exhibited high intestine values. SIP(P12) antibody levels in the tumor decreased faster than observed for SIP(F16). A difference in affinity is unlikely to be the cause for the worse targeting performance of SIP(P12), considering that its dissociation constant for the antigen was comparable with the one of the F16 antibody. Other variables that may influence targeting of the presented antibodies include antigen-related factors, such as specificity, abundance, localization, or stability. Circulating antigen levels and antibody-related factors (e.g., breathing of the VH-VL interface and stickiness) may also contribute to different *in vivo* tumor-targeting performances.

The specificity of the large isoform of tenascin-C has been documented in several studies (26, 30, 31), warranting a clinical use of human antibodies specific to the large isoforms of tenascin-C. By locoregional application of a radiolabeled murine antibody specific to the large isoform of TnC, Zalutsky et al. have observed impressive curative effects in glioma patients (34). However, brachytherapy is not possible for the treatment of disseminated disease. In view of its excellent tissue distribution, F16 is compatible with i.v. administration and is a promising antibody for the treatment of disseminated tumors given that the tissue distribution of F16 in humans is comparable with that in mice. Some of the immediate applications of the scFv(F16) include the development of fusion proteins with cytokines (e.g., interleukin-2, interleukin-12, tumor necrosis factor-α, and IFN-γ; refs. 15–18) and radioimmunotherapeutic applications (24) or possibly other antibody derivatives (6, 19, 21). The therapeutic results of the ongoing clinical trials with ^{131}I-SIP(L19) and scFv(L19)-IL2, if efficacious, will provide an enormous motivation for pursuing similar clinical development activities with F16 derivatives, particularly for cancer types, such as lung, breast, or prostate, which express high levels of TnC-A1 (Fig. 4) but are only weakly positive for EDB (12).

References

1. Forero A, Lobuglio AF. History of antibody therapy for non-Hodgkin's lymphoma. Semin Oncol 2003; 30:1–5.
2. Neri D, Bicknell R. Tumour vascular targeting. Nat Rev Cancer 2005;5:436–46.
3. Adams GP, Weiner LM. Monoclonal antibody therapy of cancer. Nat Biotechnol 2005;23:1147–57.
4. Weiner LM, Carter P. Tunable antibodies. Nat Biotechnol 2005;23:556–7.
5. Carter P. Improving the efficacy of antibody-based cancer therapies. Nat Rev Cancer 2001;1:118–29.
6. Wu AM, Senter PD. Arming antibodies: prospects and challenges for immunoconjugates. Nat Biotechnol 2005;23:1137–46.
7. van Der Veen AH, ten Hagen TL, de Wilt JH, van Ijken MG, Eggermont AM. An overview on the use of TNF-α: our experience with regional administration and developments towards new opportunities for systemic application. Anticancer Res 2000;20:3467–74.
8. Brack SS, Dinkelborg LM, Neri D. Molecular targeting of angiogenesis for imaging and therapy. Eur J Nucl Med Mol Imaging 2004;31:1327–41.
9. Pini A, Viti F, Santucci A, et al. Design and use of a phage display library. Human antibodies with subnanomolar affinity against a marker of angiogenesis eluted from a two-dimensional gel. J Biol Chem 1998; 273:21769–76.
10. Zardi L, Carnemolla B, Siri A, et al. Transformed human cells produce a new fibronectin isoform by preferential alternative splicing of a previously unobserved exon. EMBO J 1987;6:2337–42.
11. Castellani P, Viale G, Dorcaratto A, et al. The fibronectin isoform containing the ED-B oncofetal domain: a marker of angiogenesis. Int J Cancer 1994;59:612–8.
12. Kaczmarek J, Castellani P, Nicolo G, et al. Distribution of oncofetal fibronectin isoforms in normal, hyperplastic and neoplastic human breast tissues. Int J Cancer 1994;59:11–6.
13. Tarli L, Balza E, Viti F, et al. A high-affinity human antibody that targets tumoral blood vessels. Blood 1999; 94:192–8.
14. Santimaria M, Moscatelli G, Viale GL, et al. Immunoscintigraphic detection of the ED-B domain of fibronectin, a marker of angiogenesis, in patients with cancer. Clin Cancer Res 2003;9:571–9.
15. Carnemolla B, Borsi L, Balza E, et al. Enhancement of the antitumor properties of interleukin-2 by its targeted delivery to the tumor blood vessel extracellular matrix. Blood 2002;99:1659–65.
16. Ebbinghaus C, Ronca R, Kaspar M, et al. Engineered vascular-targeting antibody-interferon-γ fusion protein for cancer therapy. Int J Cancer 2005; 116:304–13.
17. Halin C, Gafner V, Villani ME, et al. Synergistic therapeutic effects of a tumor targeting antibody fragment, fused to interleukin 12 and to tumor necrosis factor α. Cancer Res 2003;63:3202–10.
18. Halin C, Rondini S, Nilsson F, et al. Enhancement of the antitumor activity of interleukin-12 by targeted delivery to neovasculature. Nat Biotechnol 2002;20: 264–9.
19. Nilsson F, Kosmehl H, Zardi L, Neri D. Targeted delivery of tissue factor to the ED-B domain of fibronectin, a marker of angiogenesis, mediates the infarction of solid tumors in mice. Cancer Res 2001; 61:711–6.
20. Birchler M, Viti F, Zardi L, Spiess B, Neri D. Selective targeting and photocoagulation of ocular angiogenesis mediated by a phage-derived human antibody fragment. Nat Biotechnol 1999;17:984–8.
21. Fabbrini M, Trachsel E, Soldani P, et al. Selective occlusion of tumor blood vessels by targeted delivery of an antibody-photosensitizer conjugate. Int J Cancer 2006;118:1805–13.
22. Heinis C, Alessi P, Neri D. Engineering a thermostable human prolyl endopeptidase for antibody-directed enzyme prodrug therapy. Biochemistry 2004;43: 6293–303.
23. Borsi L, Balza E, Bestagno M, et al. Selective targeting of tumoral vasculature: comparison of different formats of an antibody (L19) to the ED-B domain of fibronectin. Int J Cancer 2002;102:75–85.
24. Berndorff D, Borkowski S, Sieger S, et al. Radioimmunotherapy of solid tumors by targeting extra domain B fibronectin: identification of the best-suited radioimmunoconjugate. Clin Cancer Res 2005;11:7053–63s.
25. Menrad A, Menssen HD. ED-B fibronectin as a target for antibody-based cancer treatments. Expert Opin Ther Targets 2005;9:491–500.
26. Borsi L, Carnemolla B, Nicolo G, et al. Expression of different tenascin isoforms in normal, hyperplastic and neoplastic human breast tissues. Int J Cancer 1992; 52:688–92.
27. Murphy-Ullrich JE, Lightner VA, Aukhil I, et al. Focal adhesion integrity is downregulated by the alternatively spliced domain of human tenascin. J Cell Biol 1991;115:1127–36.
28. Hindermann W, Berndt A, Borsi L, et al. Synthesis and protein distribution of the unspliced large tenascin-C isoform in oral squamous cell carcinoma. J Pathol 1999;189:475–80.
29. Kusagawa H, Onoda K, Namikawa S, et al. Expression and degeneration of tenascin-C in human lung cancers. Br J Cancer 1998;77:98–102.
30. Katenkamp K, Berndt A, Hindermann W, et al. mRNA expression and protein distribution of the unspliced tenascin-C isoform in prostatic adenocarcinoma. J Pathol 2004;203:771–9.
31. Hauptmann S, Zardi L, Siri A, et al. Extracellular matrix proteins in colorectal carcinomas. Expression of tenascin and fibronectin isoforms. Lab Invest 1995; 73:172–82.
32. Carnemolla B, Castellani P, Ponassi M, et al. Identification of a glioblastoma-associated tenascin-C isoform by a high affinity recombinant antibody. Am J Pathol 1999;154:1345–52.
33. Castellani P, Dorcaratto A, Siri A, Zardi L, Viale GL. Tenascin distribution in human brain tumours. Acta Neurochir (Wien) 1995;136:44–50.
34. Reardon DA, Akabani G, Coleman RE, et al. Phase II trial of murine (131)I-labeled antitenascin monoclonal antibody 81C6 administered into surgically created resection cavities of patients with newly diagnosed malignant gliomas. J Clin Oncol 2002;20:1389–97.
35. Riva P, Franceschi G, Frattarelli M, et al. ^{131}I radioconjugated antibodies for the locoregional radioimmunotherapy of high-grade malignant glioma-phase I and II study. Acta Oncol 1999;38:351–9.
36. Rizzieri DA, Akabani G, Zalutsky MR, et al. Phase 1 trial study of ^{131}I-labeled chimeric 81C6 monoclonal antibody for the treatment of patients with non-Hodgkin lymphoma. Blood 2004;104:642–8.
37. Paganelli G, Magnani P, Zito F, et al. Pre-targeted immunodetection in glioma patients: tumour localization and single-photon emission tomography imaging of [99mTc]PnAO-biotin. Eur J Nucl Med 1994;21: 314–21.
38. Paganelli G, Grana C, Chinol M, et al. Antibody-guided three-step therapy for high grade glioma with yttrium-90 biotin. Eur J Nucl Med 1999;26: 348–57.
39. Petronzelli F, Pelliccia A, Anastasi AM, et al. Improved tumor targeting by combined use of two antitenascin antibodies. Clin Cancer Res 2005;11: 7137–45s.
40. Winter G, Griffiths AD, Hawkins RE, Hoogenboom HR. Making antibodies by phage display technology. Annu Rev Immunol 1994;12:433–55.
41. Viti F, Nilsson F, Demartis S, Huber A, Neri D. Design and use of phage display libraries for the selection of antibodies and enzymes. Methods Enzymol 2000; 326:480–505.
42. Scheuermann J, Viti F, Neri D. Unexpected observation of concentration-dependent dissociation rates for antibody-antigen complexes and other macromolecular complexes in competition experiments. J Immunol Methods 2003;276:129–34.
43. Tomlinson IM, Walter G, Marks JD, Llewelyn MB, Winter G. The repertoire of human germline VH sequences reveals about fifty groups of VH segments with different hypervariable loops. J Mol Biol 1992; 227:776–98.
44. Williams SC, Frippiat JP, Tomlinson IM, et al. Sequence and evolution of the human germline V λ repertoire. J Mol Biol 1996;264:220–32.
45. Hoogenboom HR, Griffiths AD, Johnson KS, et al. Multi-subunit proteins on the surface of filamentous phage: methodologies for displaying antibody (Fab) heavy and light chains. Nucleic Acids Res 1991;19: 4133–7.
46. Silacci M, Brack S, Schirru G, et al. Design, construction, and characterization of a large synthetic human antibody phage display library. Proteomics 2005; 5:2340–50.
47. Adams M, Jones JL, Walker RA, Pringle JH, Bell SC. Changes in tenascin-C isoform expression in invasive and preinvasive breast disease. Cancer Res 2002;62: 3289–97.
48. Natali PG, Nicotra MR, Bartolazzi A, et al. Expression and production of tenascin in benign and malignant lesions of melanocyte lineage. Int J Cancer 1990; 46:586–90.
49. Hu S, Shively L, Raubitschek A, et al. Minibody: a novel engineered anti-carcinoembryonic antigen antibody fragment (single-chain Fv-CH3) which exhibits rapid, high-level targeting of xenografts. Cancer Res 1996;56:3055–61.
50. Wong JY, Chu DZ, Williams LE, et al. Pilot trial evaluating an ^{123}I-labeled 80-kilodalton engineered anticarcinoembryonic antigen antibody fragment (cT84.66 minibody) in patients with colorectal cancer. Clin Cancer Res 2004;10:5014–21.

Clinical Cancer Research

Tumor-Targeting Properties of Novel Antibodies Specific to the Large Isoform of Tenascin-C

Simon S. Brack, Michela Silacci, Manfred Birchler, et al.

Clin Cancer Res 2006;12:3200-3208.